Increased upconversion quantum yield in plasmonic structures

A. Elhalawany,[1, 2] W. E. Hayenga,[1] S. He,[3] C. Lantigua,[1] N. J. J. Johnson,[3] A. Almutairi,[3] and M. Khajavikhan,[1*]

[1]CREOL, College of Optics and Photonics, University of Central Florida, Orlando, Florida 32816-2700, USA
[2]Department of Physics, University of Central Florida, Orlando, Florida 32816, USA
[3]Skaggs School of Pharmacy and Pharmaceutical Sciences, KACST-UCSD Center of Excellence in Nanomedicine, Laboratory of Bioresponsive Materials, University of California, 9500 Gilman Dr., 0600, PSB 2270, La Jolla, San Diego, USA
*Corresponding author: mercedeh@creol.ucf.edu

ABSTRACT

Upconversion processes have found widespread applications in drug delivery, bio-imaging and solar-cells. In this paper we present a theoretical model that analyzes the impact of a plasmonic shield structure on the quantum yield of upconversion nanoparticles. We use this model to assess the efficiency of $NaYF_4$: Tm^{3+} Yb^{3+}/$NaYF_4$ core-shell nanoparticles when embedded in a polymer matrix and covered by a metallic can-like structure. We find that as a result of this specific plasmonic structure, the upconversion luminescence from NIR to UV can be increased by a factor of 30.

Keywords: Upconversion, Plasomonic cavities, Near Infrared, Ultraviolet sources

1. INTRODUCTION

Photon upconversion (UC) is an anti-stokes process in which the successive absorption of two or more photons leads to the emission of light with shorter wavelength. UC takes place in materials that often contain ions of d-block and f-block elements [1,2]. In recent years, upconversion nanoparticles (UCNPs) have attracted considerable attention due to their potential applications in a number of areas such as bio-imaging, photovoltaics, drug delivery, therapeutics, IR detection, ultraviolet sources, etc. [3]. These potential applications have driven research towards developing more efficient UC materials. For example, significant advancement has been made in synthesizing codoped UC nanocrystals in which one type of doping (sensitizer) absorbs the light and transfers it to another type of doping (activator). Moreover, appropriately shelling the upconverting nanocrystals has led to reduced quenching through surface defects and non-radiative recombination [4]. Despite these advancements, the low luminescence efficiency still remains a challenging aspect for UC systems.

While the efficiency of UC processes for individual nanoparticles is mainly governed by chemistry and synthesis techniques, in applications where several UCNPs can be encapsulated in a submicrometer size cavity, photonics and quantum optics can provide additional tools to further customize not only the upconversion emission spectra, but also the radiation pattern. Along these lines, metallic patterning schemes have been frequently suggested as ways to increase near-infrared (NIR) absorption of UC nanocrystals [5–7]. For example, a threefold enhancement of NIR absorption has been reported using gold nanoparticles in conjunction with Er^{3+}_ doped $NaYF_4$ UCNPs [8]. However, due to direct contact of UCNPs and the metal, the emission in such structures is ultimately subject to quenching. In this manuscript, we will show that the efficiency of the UC processes are enhanced by more than an order of magnitude if nanoscale metal cavities are employed. Our study is carried out for amalgams of β-phase $NaYF_4$: Tm^{3+} Yb^{3+} –$NaYF_4$ core–shell nanoparticles encapsulated in a cylindrical plasmonic nanocavity. In this case, as a result of the presence of the nanocavity, both the absorption characteristics as well as the local density of states (LDOS) are modified. The resulting effects are then integrated in the rate equation model that studies the emission spectrum. Finally, the impact of these nanocavities on the emission directionality of the UC systems is discussed.

Plasmonics: Metallic Nanostructures and Their Optical Properties XII, edited by Allan D. Boardman, Proc. of SPIE Vol. 9163, 916331 · © 2014 SPIE
CCC code: 0277-786X/14/$18 · doi: 10.1117/12.2061910

2. PLASMONIC CAVITY

Figure 1 depicts a schematic of our proposed plasmonic cavity. The nanoparticles are embedded in a thin film of polymethyl methacrylate (PMMA) polymer [9]. UC containing nanocavities are then formed by patterning cylindrical rods which are subsequently shelled by aluminum tubes as shown in Fig. 1(a). In this arrangement, the emission will be less affected by quenching as the UCNPs are dispersed in PMMA which separates them from the metallic tube. This UC containing cylindrical nanocavity is assumed to have a radius of 150 nm and a height of 200 nm. In our analysis, the radial thickness of the aluminum tube is 50 nm. The goal here is to maximize the conversion from the NIR band to the ultraviolet (UV) band. Due to its low dissipation loss at UV bands relative to gold and silver, aluminum has been chosen. As for visible bands, it will be more appropriate to select gold tubes.

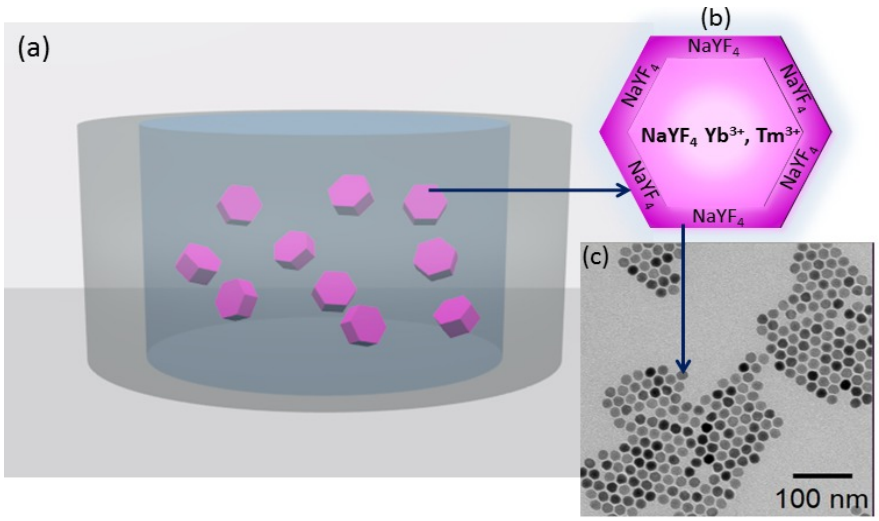

Figure 1. (a) Shows a schematic of the nanocavity containing upconversion β-phase $NaYF_4$: Tm^{3+} Yb^{3+} -$NaYF_4$ core-shell nanoparticles. (b) Shows a schematic for the upconversion β-phase $NaYF_4$: Tm^{3+} Yb^{3+} -$NaYF_4$ core-shell nanoparticles. (c) Tunneling electron microscope image for the β-phase $NaYF_4$: Tm^{3+} Yb^{3+} -$NaYF_4$ core-shell nanoparticles.

3. NUMERICAL ANALYSIS

Given UC is a nonlinear process, increasing the NIR absorption (effectively increasing the incident power delivered to the nanoparticles) can increase the conversion efficiency to all spectral bands. The ground state absorption (GSA) of the activator ions, beside the excited state absorption (ESA), and stimulated emission (STE) processes in the sensitizer ions linearly scale with the illuminating photon flux density. These in turn impact the whole dynamics of the UC system.

The analysis for the absorption of the 980 nm NIR excitation is performed using finite element methods (FEM). The net absorption coefficient of the polymer containing UCNPs is considered to be 5 cm^{-1} [5]. Figure 2 demonstrates the NIR absorption difference from a bare cylinder (Fig. 2a) to that of the aluminum-tubed cylinder (Fig. 2b). In these figures the absorption profile is plotted in cylindrical coordinates r and z. In both cases, the capsules are illuminated by a linearly polarized plane wave, incident from the bottom. For the aluminum-shelled structure, the FEM simulation predicts an overall enhancement factor (in the UCNP containing polymer region) of more than three in the absorption in comparison to the unshelled cylinder.

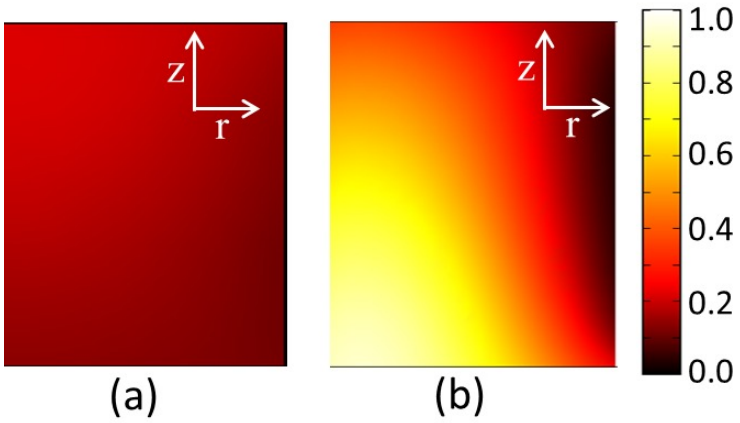

Figure 2 Normalized absorbed power density (watt per volume) at a wavelength of 980 nm (NIR) in the polymer region by (a) UCNPs- embedded in a bare cylindrical cavity (b) The same structure when surrounded by an Al ring with a thickness of 50 nm as depicted in Fig. 1.

The LDOS at the resonant transition frequencies are affected by the presence of the proposed plasmonic shielding. The transition probability P_{if} of the spontaneous emission process at a frequency ω_{if} is governed by Fermi's golden rule and is directly proportional to the LDOS $\rho(\vec{r},\omega_{if})$ at position $\vec{r}$ and is given by,

$$P_{if}(\vec{r},\omega_{if}) = \frac{2\pi}{\hbar}\left|M_{if}\right|^2 \rho(\vec{r},\omega_{if}), \qquad (1)$$

where M_{if} represents a dipole transition matrix element [10]. Since the output luminescence at frequency ω_{if} is linearly proportional to the rate of the associated transition, in principle, by engineering the LDOS, one can alter the transition rates in order to increase the UC quantum yield at the spectral band of interest.

Figure 3 shows the LDOS for the two aforementioned UC arrangements (cylinder without and with the aluminum shell). The simulations are carried out for an ensemble of ten randomly oriented dipoles, placed in random locations within the polymer

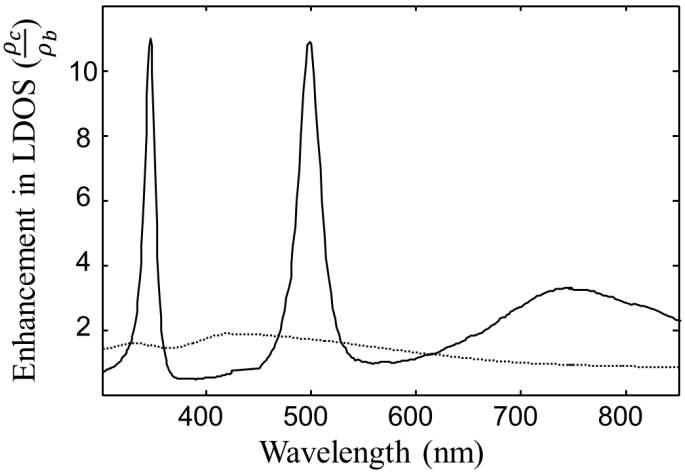

Figure 3 Enhancement factor of the LDOS for UCNPs- embedded in a bare polymer cylindrical cavity (dashed line), and for the same structure when surrounded by an aluminum ring with a thickness of 50 nm (solid line). $\boldsymbol{\rho_b}$ and $\boldsymbol{\rho_c}$ are the local density of states in the bulk and in the cavity, respectively.

cylinder. Figure 3 displays no marked features for the bare cylinder, the aluminum-shelled structure shows more than an 11-fold improvement in the LDOS at the UV spectral band centered at 360 nm.

Through the above two mechanisms, the proposed nanoscale plasmonic cavity alters the dynamical response of the UCNPs. This can be modeled by the rate equations adapted to these systems. The rate equations to these $NaYF_4$: Tm^{3+}, Yb^{3+} based systems are given as follows,

$$\dot{n} = (M_{GSA} + M_{ESA} + M_{STE} + M_{MP} + M_{SPE})n + [ET], \qquad (2)$$

where vector n represents populations of the involved energy bands which includes $^2F_{7/2}$ and $^2F_{5/2}$ levels of the activator (Yb^{3+}) ions, and $^3H_6$, $^3F_4$, $^3H_5$, $^3H_4$, $^3F_2$, $^3F_3$, $^1G_4$, $^1D_2$ levels of the sensitizer (Tm^{3+}), as shown in Fig. 4. The ground state absorption matrix (M_{GSA}) defines transitions between $^2F_{7/2}$ and $^2F_{5/2}$ of the activator ions, and likewise the excited state absorption matrix (M_{ESA}) describes the transitions between the sensitizer's upper levels with energy separation corresponding to the excitation frequency. The stimulated emission (M_{STE}) matrix denotes the rate of stimulated transitions at the excitation wavelength of 980 nm. The non-radiative transitions between energy bands enabled by multiple phonons exchange between the host crystal and the sensitizer ions is represented by the multi phonon matrix (M_{MP}). Finally, the spontaneous emission matrix (M_{SPE}) characterizes the spontaneous radiative transitions between all energy bands involved. In addition to the above linear processes, a total of eight nonlinear processes are considered in our model that governs the energy transfer between the sensitizer and activator ions ($[ET]$). Half of these processes are UC energy transfers while the other half of them are cross relaxation mechanisms. The near-field dipole-dipole interactions are responsible for the energy transfer between activator and sensitizer ions. The parameters used in our analysis are obtained from available literature [11-13].

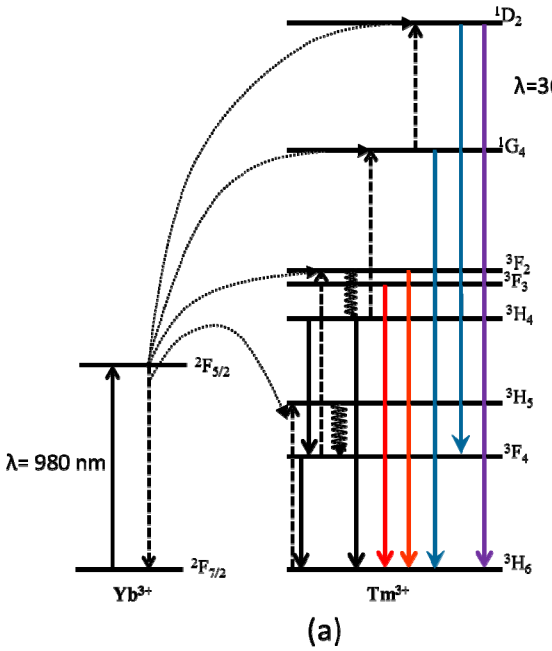

Wavelength (nm)	Electronic transition	Transition probability
1800	$^3F_4 \rightarrow {}^3H_6$	13%
1470	$^3H_4 \rightarrow {}^3F_4$	4%
980	$^2F_{5/2} \rightarrow {}^2F_{7/2}$	46%
800	$^3H_4 \rightarrow {}^3H_6$	35%
660	$^3F_2 \rightarrow {}^3H_6$	0.2%
645	$^3F_3 \rightarrow {}^3H_6$	
475	$^1G_4 \rightarrow {}^3H_6$	1.1%
450	$^1D_2 \rightarrow {}^3F_4$	0.4%
360	$^1D_2 \rightarrow {}^3H_6$	0.04%

(b)

Figure 4 (a) Schematic energy level diagram, upconversion excitation and emission lines for a $NaYF_4$ Yb^{3+}, Tm^{3+} system. (c) A table summarizing the emission wavelengths, corresponding transitions, and the transition probabilities of the upconversion nanoparticles.

The rate equation system is numerically integrated using the Runge–Kutta method. The output luminescence at the frequency of interest is then calculated by multiplying the population of an initial level with the decay rate accompanied with the corresponding final level. After such simplification, it is possible to find the full emission spectrum of UC nanoparticle systems.

Figure 5 illustrates the spectrum of the two previously mentioned $NaYF_4$: Tm^{3+} Yb^{3+} UCNP systems. The dotted line represents the luminescence spectrum of nanocrystals in the polymer rod while the solid line is the luminescence spectrum of UCNPs in the aluminum tubed nanocavity of Fig. 1. As shown in this figure, the presence of the nanocavity results in a 34-fold increase in the luminescence emission at the targeted UV spectral band centered at 360 nm. The simulation is done for an excitation intensity of 1000 W/m^2 with a spectral broadening of 2.6 nm at a wavelength of 980 nm. All emission signatures corresponding to the resonant transition frequencies in the Tm^{3+} and Yb^{3+} are assumed to have identical Lorentzian lineshape, while the transition

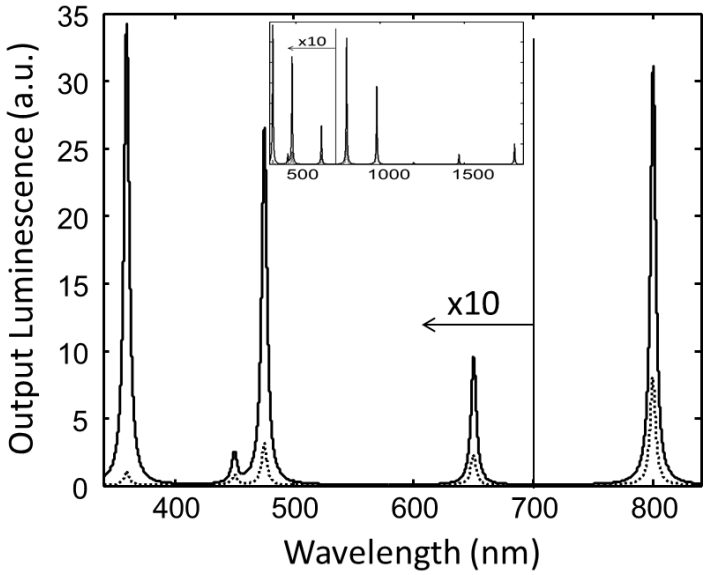

Figure 5 Spectrum of the $NaYF_4$: Tm^{3+} Yb^{3+} UC nanoparticles. The dotted line represents the luminescence spectrum of UCNPs in a polymer rod, while the solid line depicts the luminescence spectrum of UCNPs in the aluminum tubed nanocavity of Fig. 1. The inset shows the full spectrum (340-1840 nm). Below 700 nm, the emission is magnified by an order of magnitude for demonstration purposes.

probability is only affecting the peak values. The doping concentration of Tm^{3+} and Yb^{3+} ions is 0.3% and 25%, respectively.

Beside the improvement in UC efficiency at the demanded spectral band, placing UCNPs in appropriately engineered nanocavities can modify their radiation pattern. Figure 6 displays the spatial structure of the electromagnetic (optical) mode maintained by the above cavity at a wavelength of 360 nm. For such mode, the quality factor is 21. No confined cavity mode could be recognized at higher emission wavelengths in the visible and NIR wavelengths. The formation of this mode entails that unlike the omnidirectional radiation from an ensemble of randomly oriented UC nanoparticles, the emission from the UCNP nanocavity possesses higher spatial coherence and therefore can be more efficiently delivered to a target.

4. CONCLUSION

In conclusion, we propose a plasmonic nanocavity that can alter the emission spectra of upconversion nanocrystals. Our nanocavity provides up to a 34-fold increase in emission at the 360nm centered UV spectral band. This enhancement is a direct consequence to the modified NIR absorption and local photonic density of states in the presence of the proposed nanocavity. This analysis is applied to the $NaYF_4$ core shell nanocrystals codoped by Tm^{3+} and Yb^{3+}, nevertheless the illustrated results are generic. The proposed method can be utilized in a variety of upconversion systems by optimizing the cavity size, metallic tube thickness, and by selecting a fitting metal for tubing. Likewise, this analysis is valid for different spectral bands. In the proposed geometry, the nanoparticles are not in direct contact with the metal, quenching, which is generally considered the most challenging limitation in using plasmonics resonances for upconversion enhancement, is of no concern. The upconversion containing nanocavities as suggested in this letter could be potentially useful in drug delivery and release at target applications [14].

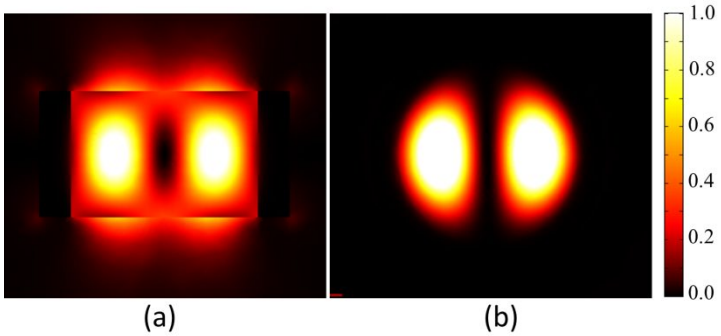

Figure 6 A confined electromagnetic mode in the UCNP-polymer system surrounded by an aluminum tube. The cavity supports a plasmonic mode with a quality factor of 21 at UV (360 nm). The side and top views (taken at the center) of the $|E_{norm}|^2$ of the UV mode are depicted in (a) and (b), respectively.

REFERENCES

1. N. Bloembergen, Phys. Rev. Lett. **2**, 84 (1959).
2. F. Auzel, Chem. Rev. **104**,139 (2004).
3. F. Wang, R. Deng, J. Wang, Q. Wang, Y. Han, H. Zhu, C. Xueyuan and X. Liu, Nat. Mater. **10**, 968 (2011).
4. F. Wang, D. Banerjee, Y. Liu, X. Chen, and X. Liu, Analyst **135**, 1839 (2010).
5. S. Schietinger, T. Aichele, HQ Wang, T. Nann, and O. Benson. Nano Lett. **10** 134 (2009).
6. Sun, Q. C., Haridas Mundoor, J. C. Ribot, V. Singh, I. I. Smalyukh, and P. Nagpal. Nano Letters **14**, 101 (2013).
7. H. Zhang, Y. Li, I. A. Ivanov, Y. Qu, Y. Huang, and X. Duan, Angew. Chem. Int. Ed. **49**, 2865 (2010).
8. S. Fischer, J. C. Goldschmidt, P. Löper, G. H. Bauer, R. Brüggemann, K. Krämer, D. Biner, M. Hermle, and S. W. Glunz, J. Appl. Phys. **108** 044912 (2010).
9. A. Shalav, B. S. Richards, and M. A. Green, Sol. Energy Mater. Sol. Cells **91**, 829 (2007)
10. E. M. Purcell, Phys. Rev. **69** 681 (1946)
11. S. Fischer, H. Steinkemper, P. Löper, M. Hermle, and J. C. Goldschmidt, J. Appl. Phys. **111** 013109 (2012).
12. S. E. Ivanova, A. M. Tkachuk, A. Mirzaeva and F. Pellé. Opt. Spectrosc. **105** 228 (2008).
13. Q. Nie, X. Li, S. Dai, T. Xu, Z Jin, X. Zhang. J. Lumin. **128** 135 (2008).
14. M. L. Viger, M. Grossman, N.. Fomina, and A. Almutairi, Adv. Mater. **25**, 3733 (2013).